ISSN:2790-1688 Volume-15-(2025)

Fiber-Based Flexible Zinc-Ion Batteries: Recent Advances and Future Perspectives

Zian Feng

College of Textiles and Clothing, Nantong University, Nantong, Jiangsu 226000, China

seraphinasouth@gmail.com

Abstract. Fiber-based flexible zinc-ion batteries (FFZIBs) represent a new class of next-generation energy storage systems distinguished by their low mass, outstanding mechanical deformability, superior textile compatibility, and inherent operational safety. These unique attributes make them particularly suitable for wearable electronics and smart textile applications. Nevertheless, the practical deployment of FFZIBs is still hindered by multiple intrinsic challenges, such as inadequate energy density, uncontrolled Zn dendrite formation, poor electrolyte durability, and difficulties in scalable production. This review first elucidates the underlying electrochemical mechanisms of aqueous zinc-ion batteries (AZIBs) and subsequently provides a comprehensive overview of the fabrication strategies employed for constructing fiber-based flexible architectures. Subsequently, recent progress in performance enhancement strategies is comprehensively discussed, with emphasis on cathode material design, anode structure engineering, and gel electrolyte optimization. Finally, key challenges and future directions for FFZIBs are highlighted, emphasizing structural design, material and electrolyte optimization, interfacial regulation, and encapsulation, which are critical for their practical use in wearable energy systems.

Keywords: aqueous zinc-ion batteries; fiber-based architectures; zinc dendrite suppression; interfacial side reactions; flexible and wearable energy devices.

1. Introduction

In recent years, the swift advancement of smart wearable devices has driven sustained innovation and development in associated technological fields. As a core component, the battery critically determines the comfort, operational lifetime, and functional versatility of wearable electronics through its lightweight design, mechanical flexibility, and high energy density. Conventional rigid batteries, however, fail to meet the stringent material requirements of next-generation wearable systems, which demand flexibility, low weight, and biocompatibility. As a result, flexible batteries have garnered growing research attention, with efforts directed toward achieving a synergistic balance of high energy density, mechanical robustness, and long-term electrochemical durability to satisfy the stringent requirements of practical wearable electronics. Fibers, featuring stretchability, small diameters, high aspect ratios, superior bending elasticity, and excellent mechanical strength, play indispensable roles in diverse functional applications. The continuous enhancement of fiber performance and the refinement of textile architectures have fostered the emergence of intelligent fibers and smart textiles. Benefiting from their lightweight nature, breathability, and adaptability to complex mechanical deformations, these intelligent fiber-based systems hold remarkable advantages and broad application potential in flexible batteries and smart wearable technologies.

Fiber-based batteries are flexible energy storage devices constructed from one-dimensional or quasi-one-dimensional fiber architectures, in which electrode materials, current collectors, and electrolytes are integrated onto a fiber scaffold to achieve efficient energy storage. They combine high specific surface area, mechanical flexibility, low weight, and excellent weavability, resulting in favorable electrochemical performance and robust mechanical stability. The structural designability and integrability of these systems allow adaptation to multidimensional configurations and complex application scenarios, meeting the demands of flexible electronics for miniaturization, deformability, and structural compatibility. Fiber ZIBs have recently attracted significant attention as a promising category of fiber batteries, owing to their intrinsic safety, low cost, and environmental compatibility. By employing aqueous electrolytes, they markedly reduce flammability and environmental hazards

compared with lithium-ion batteries, meeting the stringent safety and biocompatibility requirements of wearable electronics. Furthermore, zinc anodes offer high theoretical capacity and low redox potential, providing a material foundation for achieving high energy density and long cycling stability. Structurally, fiber ZIBs integrate the high ionic conductivity and inherent safety of aqueous zinc-ion systems with excellent strain tolerance, enabling them to withstand bending, twisting, and even weaving deformations.

This review first introduces the fundamental principles of AZIBs, followed by an overview of fabrication strategies for fiber-based flexible batteries. It then reviews recent advances in FFZIBs, focusing on cathode material design, anode structural optimization, and gel electrolyte development. Finally, the review highlights key challenges and future research directions in this field.

2. Structure and Working Principle of AZIBs

AZIBs are rechargeable systems employing metallic zinc anodes and aqueous electrolytes as ion-conducting media. Fiber ZIBs are composed of a zinc anode, a zinc-storage cathode, an electrolyte, and a separator (Figure 1). During discharge, zinc at the anode undergoes oxidation to produce Zn^{2+} ions and electrons. The electrons pass through the external circuit, while the Zn^{2+} ions migrate through the electrolyte and are stored at the cathode. During charging, Zn^{2+} is released from the cathode and reduced at the anode surface, redepositing as metallic zinc and completing the reversible cycle. The separator regulates Zn^{2+} transport, preventing electrode shorting and maintaining efficient ion conduction. Cathodes are selected for structural stability and electrical conductivity, ensuring high electrochemical efficiency and prolonged cycling performance.

The energy storage mechanisms of AZIBs primarily include Zn^{2+} intercalation/deintercalation, dual-ion co-intercalation, conversion reactions, and organic coordination processes. Among these, Zn^{2+} intercalation is widely recognized as a representative mechanism, with cathodes featuring layered or tunnel structures demonstrating high reversibility and structural stability[1]. During discharge, the cathode accepts electrons from the external circuit while Zn^{2+} ions migrate from the electrolyte to intercalate into the cathode lattice. During charging, the intercalated Zn^{2+} ions are extracted back into the electrolyte, accompanied by electron release from the cathode.This intercalation/deintercalation process can be described by the following reaction equation:

$$Zn \leftrightarrow Zn^{2+} + 2e^{-} \quad (1)$$

$$M + xZn^{2+} + 2e^{-} \leftrightarrow Zn_xM \quad (2)$$

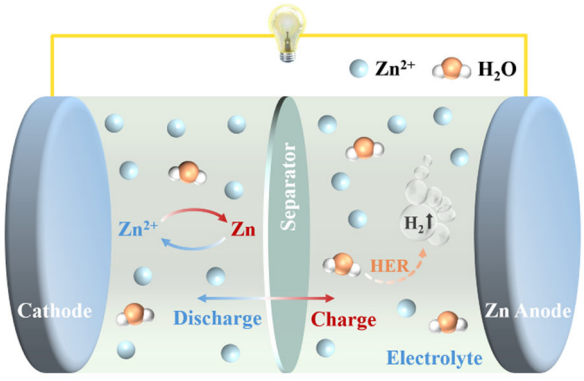

Figure 1. Working principle of AZIBs.

3. Preparation of Fiber-Based Flexible Batteries

3.1 Electrospinning Technique

Electrospinning technology has become a widely used method for fabricating nanofibers owing to its low cost, simple operation, and strong controllability[2]. This technique employs a high-voltage

electric field to extrude polymer solutions or melts from a nozzle, where the jet is stretched under the electric field to form nanometer-scale fibers. The fibers possess a large specific surface area, favorable electrical conductivity, and outstanding mechanical strength, which collectively render them promising candidates for use as electrode materials in flexible batteries. Electrospinning not only enables precise control over fiber diameter and structure but also allows large-scale production, meeting the requirements of flexible electronic devices for high performance and long-term stability. By adjusting process parameters such as applied voltage, flow rate, and collection distance, the fiber morphology can be optimized to enhance the battery's capacity, cycling stability, and charge-discharge performance[3]. Moreover, electrospinning can be employed to fabricate composite fiber electrodes, further improving the electrochemical properties of the battery. Yang et al.[4] utilized electrospinning to prepare flexible carbon-based fiber electrodes. The polymer precursor solution was stretched into nanofibers under a high-voltage electric field and subsequently converted into conductive structures through thermal treatment. The resulting electrodes exhibited tunable porous or core-shell architectures, with fiber morphology influenced by voltage, flow rate, and environmental conditions. This binder-free approach produced electrodes combining excellent flexibility and structural stability, demonstrating their suitability for high-performance AZIBs.

3.2 In-Situ Growth Technique

The in-situ growth technique enables the direct growth of electrode materials on conductive fibers, eliminating the need for electrochemically inactive additives and thereby enhancing electrode performance and stability[5]. This method typically employs hydrothermal synthesis, solution chemistry, electrochemical deposition, or vapor deposition to reduce or deposit precursor materials onto the fiber surface under specific conditions, forming the desired electrode materials[6]. Guo et al.[7] constructed MnO_2@MXene composite electrodes on carbon nanotube fibers via a two-step in-situ process, in which MnO_2 was formed through electrochemical deposition. The electrode achieved a volumetric capacitance of 371.1 F cm^{-3} and retained 86.3% capacity over 10,000 cycles, while precise control of its morphology, structure, and thickness simultaneously enhanced both electrochemical performance and device flexibility. As the electrode is directly anchored onto the fiber substrate, both mechanical robustness and flexibility are improved, making this approach particularly suitable for wearable and flexible electronic devices[8].

3.3 Surface Coating Technique

Surface coating represents an effective strategy distinguished by its simplicity, low cost, and scalability, and is widely applied in the preparation of fiber-based flexible batteries. In this approach, active electrode materials, conductive carbon additives, and binders are blended in suitable ratios to form a uniform slurry, which is subsequently deposited onto flexible fiber substrates. This process effectively improves the electrochemical performance of the electrodes while preserving their mechanical flexibility.[9]. The conductive carbon materials ensure good electrical contact, whereas the binder strengthens the adhesion among the active materials, conductive agents, and current collector, thereby improving the mechanical strength and stability of the electrode[10]. Zhang et al.[11] coated a pseudocapacitive polymer, polypyrrole (PPy), onto nanostructured MnO_2 to fabricate uniform fiber electrodes based on MnO_2 prepared using 20 μL pyridine, 7 mg SDS, and 5 min of low-temperature ultrasonication, exhibiting moderate thickness. The electrode delivered a high specific capacity of 316.0 mAh g^{-1} at 10 mA g^{-1}, exhibiting outstanding rate capability and long-term cycling stability. The key to surface coating lies in the uniformity and stability of the coating layer, which are affected by factors such as slurry viscosity, coating speed, and drying conditions. To ensure strong adhesion between the coating and substrate, chemical bonding or physical adsorption is commonly employed, and post-treatment processes such as thermal annealing or chemical crosslinking are often applied to further enhance the stability and durability of the coating[12].

3.4 Recent Advances in FFZIBs

3.5 Cathode Material Design and Optimization

The rapid advancement of FFZIBs has positioned the design and optimization of cathode materials as a pivotal factor in enhancing overall performance. Nevertheless, existing cathode materials still face multiple challenges. Firstly, the intrinsically sluggish Zn^{2+} diffusion kinetics, coupled with inadequate structural stability of the cathode lattice, often leads to dissolution or even structural collapse of the active material during cycling, resulting in a fundamental trade-off between energy density and cycle life[13]. Secondly, flexible applications demand superior mechanical toughness and interfacial stability. Traditional inorganic cathode materials are prone to microcrack formation and interfacial delamination when subjected to repeated mechanical stresses such as bending or stretching, ultimately leading to deterioration in electrochemical performance[14]. Furthermore, limited electron transport pathways hinder both high-rate capability and long-term cycling stability. This issue is particularly critical for cathodes with low intrinsic electronic conductivity, where excessive conductive additives are required, thereby diluting the active material content and reducing the overall energy density of the device[15].

Recent efforts in cathode design and optimization for FFZIBs have addressed key performance and structural challenges, yielding significant improvements in both electrochemical properties and material stability. Zhang et al.[16] fabricated a multifunctional fiber-shaped AZIB using Ti wire coated with α-MnO_2 nanoflowers as the cathode (Figure 2a). The 3D nanoflower structure provided abundant active sites and superior reaction kinetics, delivering a specific capacity of 280 mAh g^{-1}, an energy density of 396 Wh kg^{-1}, and maintaining 80.6% of its initial capacity after 300 cycles. Xu et al.[17] synthesized high-purity $H_2V_3O_8$ powder via a one-step hydrothermal method and uniformly loaded it onto carbon fiber (CF) cores through wet spinning (Figure 2b). The composite cathode achieved a maximum tensile strength of 361.9 Mpa, with pressing producing a more compact structure (Figure 2c). The assembled flexible zinc-ion fiber battery delivered a high specific capacity of 225 mAh g^{-1} at a current density of 3 A g^{-1}, together with excellent cycling stability and flexibility. Guo et al.[18] realized Ca doping through in-situ electrochemical oxidation, constructing an amorphous Ca-doped V_2O_5 nanowire array cathode (Figure 2d). The array architecture significantly enhanced Zn storage capability and volumetric capacity, while theoretical calculations revealed that Ca doping facilitated reversible transitions between amorphous and crystalline phases, thereby improving cycling stability. Cheng et al.[19] reported the fabrication of a $NiCo_2S_4$@reduced graphene oxide (rGO) core-shell composite fiber cathode via a combined surface-growth and wet-spinning strategy. The rGO shell provided efficient electron transport pathways and suppressed aggregation, while the synergistic dual-conductive network of rGO and carbon nanotubes (CNTs) further enhanced both electrochemical performance and mechanical flexibility (Figure 2e-f). The assembled fiber battery delivered a specific capacity of 175.29 mAh g^{-1} with 85.6% capacity retention after 150 charge-discharge cycles.

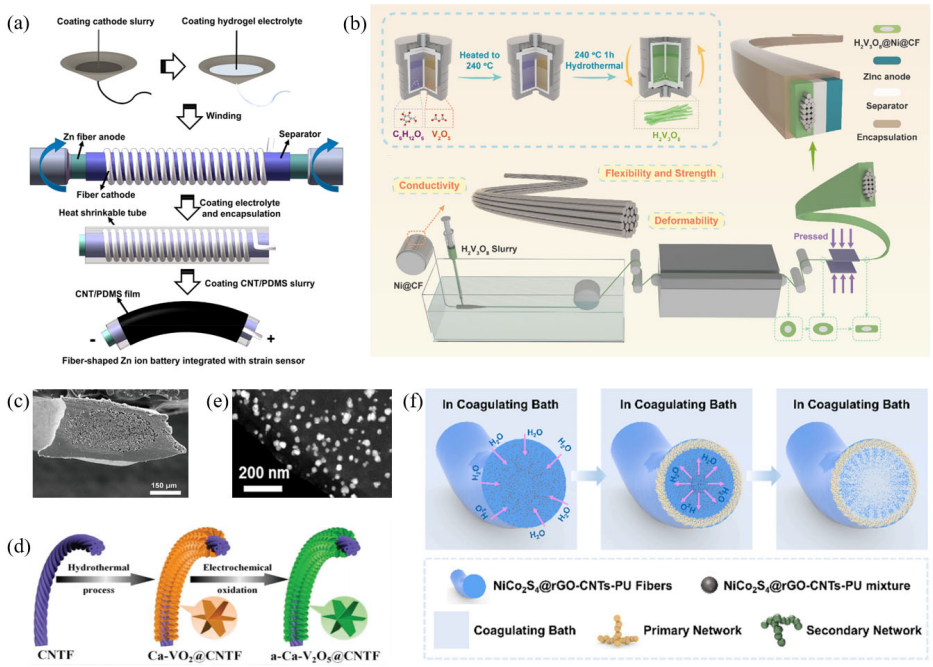

Figure 2. (a) Preparation process of multifunctional battery[16]. (b) Schematic of $H_2V_3O_8$ nanowire synthesis and $H_2V_3O_8$@Ni@CF//Zn fiber battery assembly[17]. (c) Cross-sectional SEM image of $H_2V_3O_8$@Ni@CF[17]. (d) Diagram of a-Ca-V_2O_5/carbon nanotube fiber (CNTF) synthesis procedure[18]. (e) STEM and element mapping images of $NiCo_2S_4$@rGO[19]. (f) Presumable formation mechanism of $NiCo_2S_4$@rGO-polyurethane-CNTs fiber[19].

In addition to the above studies, researchers have made numerous innovations in various material systems and fabrication processes. Subjalearndee et al.[20] fabricated a γ-MnO_2/rGO composite fiber cathode, based on wet-spinning technology (Figure 3a-b)). The rGO fibers, reduced by hydroiodic acid, were subsequently dip-coated in a mixture of γ-MnO_2, carbon black, carbon nanotubes, and xanthan gum or polyvinylidene fluoride (PVDF) as binders, the hydrophobic binders enhanced active material loading, enabling the assembled battery to achieve 230 mAh g^{-1} and retain 80% capacity over 200 cycles in an electrolyte containing 2 M $ZnSO_4$ and 0.2 M $MnSO_4$ (Figure 3c). Xia et al.[21] constructed a V_2O_5/rGO hybrid fiber cathode by regulating the rheological behavior of the spinning solution, achieving a hierarchically aligned architecture with excellent flexibility (Figure 3d-e). The V_2O_5/rGO fiber (mass ratio 10:1) exhibited a superior specific capacity of 486.03 mAh g^{-1} at 0.1 A g^{-1} and was effectively incorporated into a wearable self-powered system coupled with a GaAs solar cell, achieving an overall energy conversion efficiency of 9.80%. Li et al.[22] fabricated a FFZIB and deposited a poly(3,4-ethylenedioxythiophene):poly(styrene sulfonate) (PEDOT:PSS) protective layer on an activated cobalt hydroxide cathode [A-$Co(OH)_2$] exhibiting a network of microcracks (Figure 3f-g). This coating effectively mitigated stress concentration and prevented the detachment of active materials during bending, thereby enhancing structural stability. The system achieved an energy density of 173.5 Wh kg^{-1} at a power density of 90 W kg^{-1}, exhibiting excellent mechanical stability by preserving 94.4% of its capacity over 500 bending cycles. Khumujam et al.[23] engineered a hierarchically assembled fiber cathode (P_x-V_2O_{5-x}@CoNC@MX/CF) by tuning the electronic structure through phosphorus doping and oxygen vacancy engineering and incorporating a leaf-like morphology derived from a bimetal-organic framework grown on an MXene substrate, which facilitated Zn^{2+} diffusion, enhanced material stability, and achieved 133 mWh cm^{-3} of energy and 425.2 mW cm^{-3} of power (Figure 3h-j).

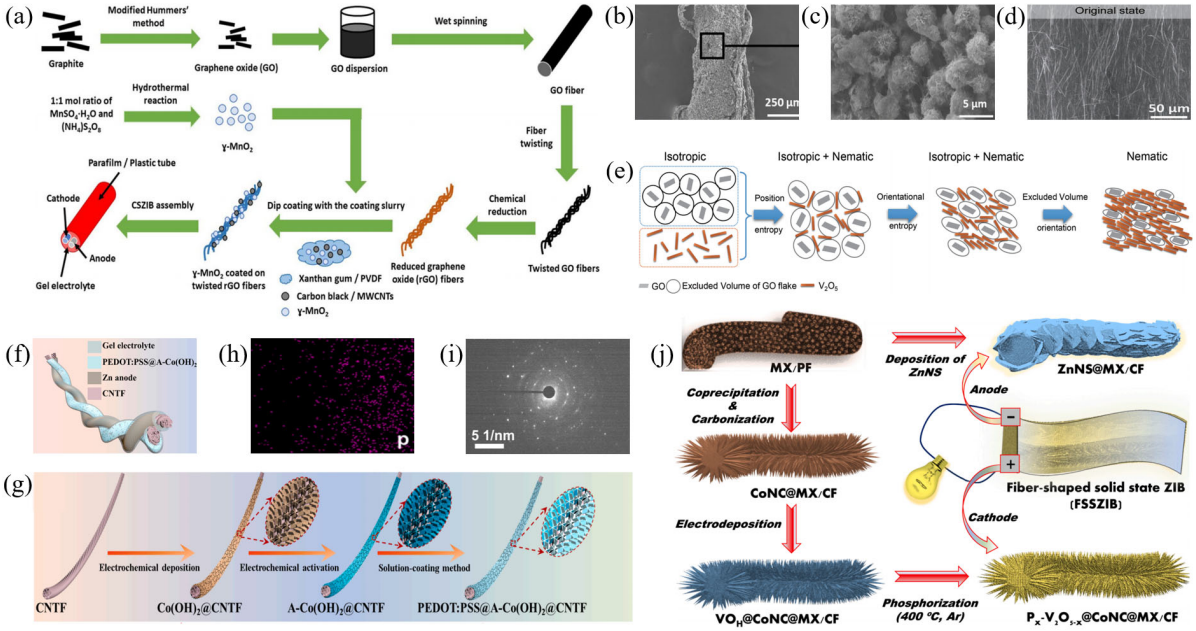

Figure 3. (a) Schematic of γ-MnO_2/rGO fiber cathode fabrication via wet spinning and dip coating[20]. SEM images of (b) γ-MnO_2/rGO-PVDF[20] and (c) coated γ-MnO_2 on rGO fibers[20]. (d) Surface SEM of as-prepared V_2O_5/rGO hybrid fiber[21]. (e) Schematic of liquid crystal phase transition during V_2O_5 nanowires and graphene oxide flakes mixing[21]. (f) Fabrication schematic of PEDOT:PSS@A-$Co(OH)_2$@CNTF[22]. (h) EDS mapping showing P element distribution[23]. (i) SAED pattern of P_x-V_2O_{5-x}@CoNC@MX/CF cathode[23]. (j) Schematic illustration of P_x-V_2O_{5-x}@CoNC@MX/CF cathode and ZnNS@MX/CF anode[23].

Pi et al.[24] synthesized a composite cathode material by in situ growing a vanadium-based metal-organic framework (MIL-47(V)) on wood fibers via a hydrothermal method, followed by high-temperature annealing under a nitrogen atmosphere to obtain carbon-coated V_2O_3 supported on carbonized wood fibers, which was assembled into a fiber-shaped AZIB. The wood fibers provided abundant nucleation sites, effectively preventing the aggregation of MIL-47(V), while the carbonized wood fibers enhanced the conductivity and structural stability of V_2O_3, thereby improving the reversibility and cycling life of vanadium oxides. Achieving 447 mAh g^{-1} at 0.1 A g^{-1}, the battery preserved 85% of its initial capacity after 2000 cycles at 5.0 A g^{-1}, indicating robust electrochemical performance. Xu et al.[25] developed a CuVO@polyaniline (PANI) composite cathode using a synergistic strategy of Cu^{2+} pre-intercalation and PANI surface coating through a combined hydrothermal and in situ polymerization process. The resulting composite featured a three-dimensional microspherical architecture assembled from two-dimensional nanosheets, exhibiting a high specific surface area and an expanded interlayer spacing of 16.1 Å, which facilitated Zn^{2+} diffusion kinetics and electron transport. The CuVO@PANI cathode achieved a specific capacity of 672.2 mAh g^{-1} at 0.1 A g^{-1} and retained 269.2 mAh g^{-1} over 2000 cycles at 6 A g^{-1}. Wu et al.[26] fabricated a self-supporting cathode by in situ growing Ni-doped V_2O_5 nanorod arrays on flexible CNTF fibers via a hydrothermal process. Ni doping induced an expansion of the V_2O_5 interlayer spacing, facilitating ionic conductivity and enhancing both reaction kinetics and structural stability during Zn^{2+} insertion/extraction. The engineered Zn/Ni-V_2O_5@CNTF cell achieved a volumetric capacity of 398.85 mAh cm^{-3} at 0.1 A cm^{-3}, demonstrating excellent cycling stability over 2000 cycles. Ding et al.[27] fabricated a flexible yarn-shaped AZIB via a conical spinning technique, using a CNT/MnO2 composite yarn to serve as the cathode and a zinc wire to act as the anode. The conical spinning process enabled uniform deposition of MnO_2 nanosheets onto the CNT fibers, forming a dense and continuous network that significantly improved ion and electron transport kinetics while effectively suppressing MnO_2 dissolution. The cathode exhibited a remarkable reversible capacity of

490.4 mAh g^{-1} at 1 A g^{-1} and achieved a high energy storage density of 559.8 Wh kg^{-1} under a power density of 4124.0 W kg^{-1}, retaining 86% of its initial capacity over 5000 cycles.

In summary, the design and optimization of FFZIB cathodes target enhanced Zn^{2+} diffusion kinetics, improved structural stability, and superior mechanical robustness. Strategies such as nanostructure engineering, elemental doping, and composite construction have effectively improved zinc storage capability, electrochemical performance, and cycling stability, while simultaneously ensuring mechanical strength and durability under flexible conditions.

3.6 Anode Design and Optimization

In FFZIBs, the anode faces critical challenges including non-uniform growth of zinc dendrites, parasitic hydrogen evolution, and electrode corrosion. The formation of zinc dendrites primarily arises from the uneven charge distribution on the anode surface, which induces localized Zn^{2+} deposition at surface protrusions and subsequently triggers dendritic growth, thereby compromising the cycling stability and safety of the battery[28]. The hydrogen evolution reaction, an inherent thermodynamic process of zinc anodes, results in capacity loss, decreased Coulombic efficiency, and gas accumulation within the cell, thereby elevating safety risks. Moreover, chemical and electrochemical corrosion at the electrode surface aggravates interfacial roughness and increases polarization resistance, further hindering uniform Zn^{2+} deposition[29].

At present, various anode design strategies have been developed to improve the uniformity of zinc deposition and the cycling stability of FFZIBs. Shen et al.[30] fabricated a fiber-shaped AZIB using a hierarchical deposition framework anode (Figure 4a). By regulating the zinc deposition overpotential and binding energy, a bottom-up layered deposition of zinc was achieved, which provided sufficient space to alleviate dendrite penetration and thus prolonged battery lifespan (Figure 4b). The device maintained 89.0% of its capacity after 2000 cycles at a 5C rate. Guan et al.[31] fabricated a fiber-shaped AZIB by acid-treating carbon fiber anodes to enhance zinc affinity, coupled with an electrochemical deposition strategy to induce preferentially oriented zinc deposition (Figure 4c). This approach effectively suppressed dendrite formation and reduced nucleation overpotential. The prepared battery demonstrated a volumetric energy storage of 5.63 mWh·cm^{-3}, sustaining 90% of its capacity over 2000 cycles while preserving flexibility from 0° to 180°, and retaining 80% of its capacity after 3000 underwater cycles (Figure 4d). Zhai et al.[32] electrodeposited zinc on carbon fiber substrates followed by coating an ultrathin carbon layer to form CF@Zn@C fiber anodes (Figure 4e). This structure enhanced nucleation uniformity and conductivity, effectively suppressing dendrite growth and dead-zinc formation while improving the reversibility of Zn plating/stripping. Under 0.25 mA·cm^{-2} and 0.125 mAh·cm^{-2} conditions, the fiber anode maintained a low overpotential of about 45 mV over 200 hours of cycling. Liu et al.[33] innovatively introduced fluorescent carbon dots (CDs) rich in zinc-affinitive functional groups as a bifunctional electrolyte additive, forming an ultrathin Zn^{2+} adsorption layer on the anode surface to lower nucleation barriers and regulate interfacial ion distribution, thereby effectively suppressing zinc dendrite growth (Figure 4f-i). Stable zinc plating/stripping was sustained for 2500 hours at 1 mA·cm^{-2}, achieving an energy density of 0.17 Wh·cm^{-3} and 78.9% capacity retention after 1500 cycles.

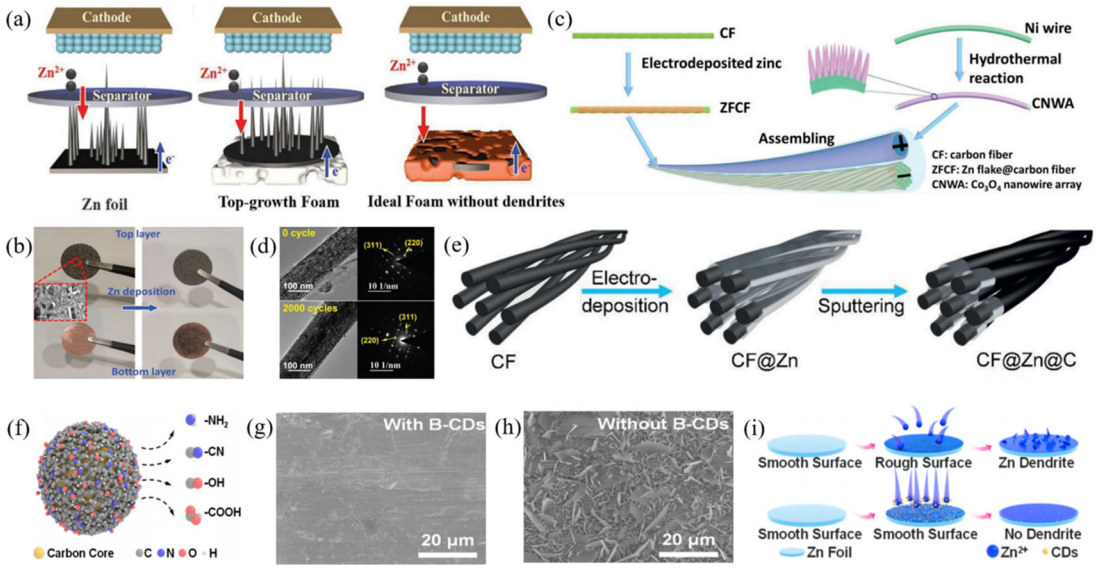

Figure 4. (a) Dendrite formation on Zn foil, CF, and ideal 3D anodes[30]. (b) Photographs of stratified deposition framework before and after Zn deposition with SEM inset[30]. (c) Schematic of aqueous fiber-shaped Zn//Co_3O_4 battery fabrication[31]. (d) TEM and SAED images of Co_3O_4 nanowires array cathode before and after 2000 cycles[31]. (e) Schematic illustration of CF@Zn@C preparation[32]. (f) Schematic illustration of Blue Fluorescent CDS (B-CDs)[33]. SEM images of (g) Zn electrode with B-CD additive[33] and (h) bare Zn[33]. (i) Mechanism diagram showing how B-CDs inhibit Zn dendrite formation[33].

In addition, Shao et al.[34] fabricated a Zn powder-based fibrous anode using a wet-spinning technique (Figure 5a). By leveraging the spinnability of carbon nanotube reinforcing materials and employing annealing treatment to regulate crystalline texture, the (002) plane was reoriented, enabling stable battery operation for over 800 hours at 1 $mA \cdot cm^{-2}$ (Figure 5b). Even after 100 torsional cycles under a 180° twisting angle, the voltage hysteresis increased by only 21.7 mV. Chen et al.[35] utilized inkjet printing to uniformly distribute Ag nanoparticles (AgNPs) on the surface of carbon cloth fibers, thereby developing an AgNP-modified carbon cloth (AgNPs@CC)/Zn fiber anode (Figure 5c). The Ag nanoparticles served as heterogeneous nucleation sites, effectively reducing Zn nucleation overpotential and promoting uniform deposition, while the reversible formation of Ag-Zn alloy enhanced cycling reversibility (Figure 5d). Moreover, the improved thermal conductivity of the fiber framework helped suppress dendrite formation at elevated temperatures. The AgNPs@CC/Zn fiber anode maintained a low voltage hysteresis of approximately 80 mV at a high current density of 10 $mA \cdot cm^{-2}$ and exhibited stable cycling performance exceeding 480 hours. Li et al.[36] constructed a FFZIB employing a Zn nanosheet (Zn NSs) array electrochemically grown on carbon nanotube (CNT) fibers to form a Zn NSs@CNT composite anode (Figure 5e). The anode sustained 71.2% of its original capacity at a 500-fold higher current density, and maintained 89.8% of its capacity after 10,000 cycles. Pu et al.[37] developed intrinsically stretchable liquid metal/polyurethane (LM/PU) composite fibers via wet spinning, onto which Zn was deposited to construct LM@Zn fiber anodes (Figure 5f-g). The high Zn affinity and alloying effect of the liquid metal induced preferential Zn deposition along the (002) crystal plane, effectively suppressing dendrite growth and improving the reversibility and anti-side-reaction capability during Zn plating/stripping. Even under 50% tensile strain, the fiber-shaped battery maintained a volumetric capacity of 139.8 $mAh \cdot cm^{-3}$ after 300 cycles, corresponding to 83.0% of its initial capacity.

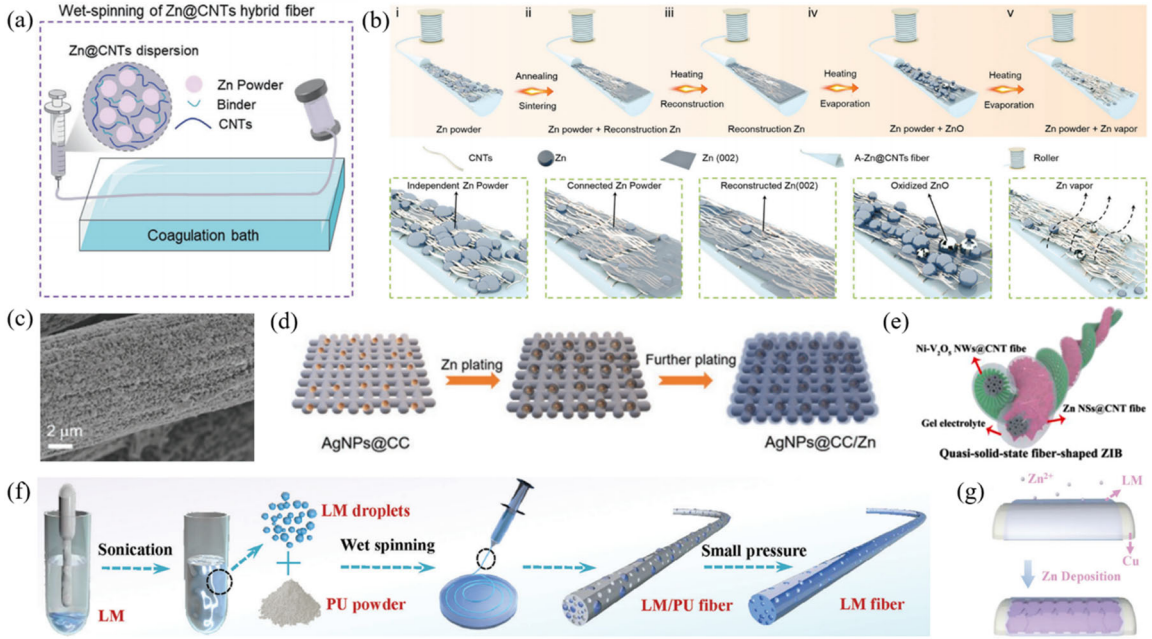

Figure 5. (a) Illustration of Zn@CNTs fiber wet-spinning and fibrous ZIBs configuration[34]. (b) Schematic of Zn (002) texture reconstruction[34]. (c) SEM image of AgNPs@CC scaffold[35]. (d) Schematic illustration of Zn deposition on AgNPs@CC scaffold[35]. (e) Illustration of the fiber-shaped quasi-solid ZIB[36]. (f) Schematic representation of LM fiber fabrication process[37]. (g) Diagram illustrating the Zn deposition behavior[37].

Wang et al.[38] constructed a fiber-shaped AZIB through the formation of a three-dimensional hybrid fibrous network on the zinc foil surface via in situ electrospinning. The battery employed a composite fibrous interfacial protection layer of $NaTi_2(PO_4)_3$ (NTP) and thermoplastic polyether-type polyurethane (TPEU), denoted as NTP@TPEU. This architecture significantly enhanced Zn^{2+} desolvation and diffusion kinetics, enabling dendrite-free Zn (002) preferential deposition. The assembled cell retained 81.6% capacity over 3000 cycles at 2 A g^{-1}, with an average Coulombic efficiency of 99.8%. Lin et al.[39] developed a fiber-shaped AZIB using non-stoichiometric copper selenide ($Cu_{2-x}Se$) as the anode material. During zinc storage, $Cu_{2-x}Se$ underwent a reversible conversion reaction from $Cu_{2-x}Se$ to Cu and ZnSe, enabling efficient Zn^{2+} storage. The battery achieved a specific capacity of 150 mAh g^{-1} at 0.5 A g^{-1} and retained 91% capacity over 20,000 cycles at 5 A g^{-1}. Cong et al.[40] engineered a flexible fiber-shaped AZIB using electrochemical deposition, constructing a nanosheet-structured zinc anode and a PANI cathode on a carbon fiber current collector. The zinc anode exhibited a three-dimensional porous morphology that promoted uniform Zn deposition and reversible stripping while suppressing dendrite formation. At 2 mA cm^{-2}, the anode attained a cumulative charge of 1000 mAh cm^{-2} with a low polarization voltage of 30 mV, maintaining 75.1% of its capacity after 1000 cycles. Lin et al.[41] further employed electrospinning to uniformly embed zinc powder into polyacrylonitrile (PAN)/PVDF fibers, forming a three-dimensional porous fibrous zinc powder anode (PF@Zn). This fibrous architecture enabled uniform Zn^{2+} flux distribution and stable nucleation, effectively suppressing dendrite growth and side reactions. The PF@Zn electrode maintained approximately 99.1% Coulombic efficiency after 240 h of cycling at 1 mA cm^{-2}, with a low nucleation overpotential of only 5.9 mV.

Overall, to address issues such as dendritic growth, uneven zinc deposition, and parasitic side reactions in fiber-shaped flexible ZIBs, multidimensional design strategies involving surface modification, structural optimization, and interfacial regulation have been developed to refine Zn deposition behavior and enhance interfacial stability. These approaches have collectively improved the cycling life, energy density, and mechanical flexibility of the devices. Notably, several studies have achieved extended cycling stability and high capacity retention under specific testing conditions.

3.7 Gel Electrolytes

Hydrogel electrolytes are a class of three-dimensional polymer network materials composed of polymer chains capable of absorbing and retaining large amounts of water, forming continuous ion transport channels, while exhibiting excellent mechanical flexibility and interfacial adhesion suitable for high-curvature and wearable device applications[42]. In FFZIBs, hydrogels regulate water molecule activity, ionic solvation structures, and interfacial compatibility, thereby facilitating Zn^{2+} transport, suppressing hydrogen evolution and zinc dendrite formation, and enhancing cycling stability and electrochemical safety[43].

Optimizing the composition and structure of hydrogel electrolytes effectively suppresses zinc dendrite growth and parasitic reactions, thereby enhancing the performance of FFZIBs. In one study, Wang et al.[44] constructed a zinc-philic polyacrylamide/sodium alginate double-network hydrogel electrolyte with strong adhesion and optimized electric field distribution, enhancing Zn^{2+} diffusion and uniform deposition to suppress dendrites and side reactions (Figure 6a-b). The zinc fiber anode demonstrated stable cycling beyond 2250 hours under a current density of 2 $mA \cdot cm^{-2}$ and a capacity density of 3 $mAh \cdot cm^{-2}$. while the 100 cm-long symmetric cell sustained operation beyond 1900 h.Moreover, the Zn‖MnO_2 preserved 80.7% of its original capacity over 1400 cycles at a 6 C rate. Xu et al.[45] fabricated a cathode-free fiber-shaped AZIB, achieving in situ manganese deposition under constant-voltage charging (Figure 6c-d). Incorporating a nanofiber-based composite hydrogel electrolyte facilitated Zn^{2+} transport, mitigated zinc dendrite growth, and suppressed parasitic side reactions. The battery delivered an energy storage of 227.08 $mWh \cdot cm^{-3}$ and a capacity of 156.48 $mAh \cdot cm^{-3}$ at 0.1 $A \cdot g^{-1}$, maintaining 76.5% capacity after 2700 cycles. The cathode-free configuration enabled uniform MnO_2 deposition and dissolution, thereby elevating the operating voltage to 1.9 V. Zhu et al.[46] incorporated oxygen-rich poly(urea-polyurethane) (OR-PUU) into polyacrylamide hydrogel to form a composite electrolyte, regulating zinc ion solvation and promoting uniform deposition with self-healing capability (Figure 6e-f). The resulting zinc symmetric cell cycled for 2000 h, and the Zn-MnO_2 full cell retained minimal capacity decay (0.009% per cycle) over 2000 cycles at 2000 mA g^{-1}. Li et al.[47] designed a bilayer hydrogel electrolyte containing lysine additives, with a highly fluid polyvinyl alcohol-Zn acetate [PVA-Zn$(AC)_2$] inner layer providing self-healing and a high-strength zinc-alginate outer layer for mechanical support, enabling confined assembly on high-curvature zinc fiber anodes (Figure 6g-i). The fiber-shaped Zn–Zn symmetric cell exhibited stable cycling for over 800 h at 0.1 Hz and 1 $mA \cdot cm^{-2}$. Meanwhile, the Zn–Prussian blue device maintained 97.7% capacity through 500 bending cycles.

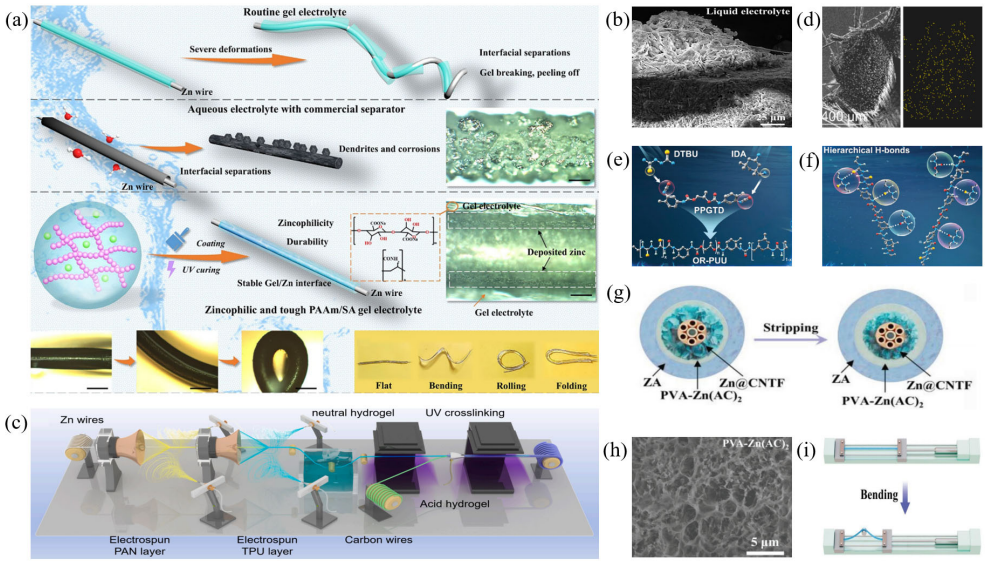

Figure 6. (a) Fabrication of fiber-shaped AZIBs[44]. (b) Cross-sectional SEM images of Zn fibers after 100 cycles[44]. (c) Illustration of Zn-Mn fiber battery preparation[45]. (d) SEM images of carbon wire cathode cross section after constant-voltage charging[45]. (e) Synthesis of OR-PUU

molecules[46]. (f) Hierarchical H-bond network enabling self-healing hydrogel electrolyte[46]. (g) Schematic of Zn@CNTF with dual-layer gel electrolyte during Zn stripping[47]. (h) Cross-sectional SEM image of PVA-Zn(AC)$_2$[47]. (i) Illustration of bending device[47].

Wang et al.[48] developed a flexible fiber-shaped solid-state ZIB with excellent anti-freezing capability. Plasma-treated carbon fiber ropes served as the conductive substrate, while the PVA hydrogel electrolyte doped with ethylene glycol (EG) and graphene oxide (GO) formed an integrated binder framework, enhancing both mechanical robustness and low-temperature electrochemical stability. GO facilitated Zn^{2+} migration via hydrogen-bonding networks, while EG lowered the freezing point and suppressed dendrite growth, enabling the battery to retain over 22% of its discharge capacity at −20°C and 91% capacity after 2000 bending cycles, with an energy density of 0.1752 mWh cm^{-1} and power density of 1.25 mW cm^{-1}. Liu et al.[49] developed a fiber-shaped flexible AZIB integrating a quasi-solid hydrogel electrolyte with enhanced ionic conductivity (0.016 S cm^{-1}), synthesized via in situ polymerization of 1-ethyl-3-vinylimidazolium dicyanamide and N,N′-methylenebisacrylamide in a zinc acetate medium. Stainless steel yarn acted as the current collector, where electro-deposited Zn nanosheets and interconnected MnO_2 nanosheets served as the anode and cathode, respectively. The in situ polymerized hydrogel was mold-injected to form a seamless encapsulation, ensuring strong interfacial integration and structural integrity. Consequently, the assembled cell achieved volumetric capacities of 2.4 mAh cm^{-3} and 4.6 mAh cm^{-3}, and volumetric energy outputs of 2.0 mWh cm^{-3} and 4.2 mWh cm^{-3} at 0 °C and 60 °C, respectively. Shim et al.[50] constructed a fiber-shaped AZIB by electrochemically depositing PANI cathode and zinc anode onto carbonized yarn, with a methanesulfonic acid (MSA)-doped PVA gel electrolyte that suppressed PANI degradation and Zn corrosion via dual-anion doping and water-trapping effects, enhancing ion conductivity and charge-transfer efficiency, and achieved 88.1% capacity retention after 2000 cycles and 92.7% after 500 bending cycles at 2.5 mm radius. Yu et al.[51] modified carbon fiber surfaces via electron spin resonance oxygen plasma and electrochemically deposited PANI, using a PVA-based hydrogel that formed a flexible electrolyte layer at low temperature, providing high ionic conductivity and mechanical flexibility, resulting in 83.96 mAh g^{-1} at 2000 mA g^{-1} and 95.39% capacity retention after 200 cycles.

Overall, hydrogel electrolytes in FFZIBs regulate ion transport and interface stability, mitigating dendrite growth and side reactions, thereby enhancing cycle life, rate performance, and structural durability, while diverse hydrogel-based optimization strategies achieve a balance between mechanical strength, flexibility, and electrochemical stability, laying the foundation for high-performance fiber-shaped energy storage devices.

4. Summary and Outlook

FFZIBs integrate mechanical flexibility, weaveability, and outstanding electrochemical performance. These attributes endow them with strong potential for application in wearable and intelligent electronic systems. This review summarizes recent advances in FFZIBs, focusing on three key aspects: cathode material design, anode structural optimization, and hydrogel electrolyte development. Despite notable progress, FFZIBS are still in the developmental stage and face several critical challenges, including insufficient energy density and cycling stability, unstable zinc anode/electrolyte interfaces, limited electrolyte durability, and reliability issues related to fabric integration and complex deformation conditions. In summary, future research aimed at enhancing the performance of FFZIBs can be directed toward the following aspects:

(1)Novel Device Structure Design: Future FFZIBs can be engineered with multidimensional architectures such as integrated, core-sheath, or helical configurations to attain a desirable equilibrium among flexibility, weaveability, and electrochemical performance. These structural strategies maximize the spatial utilization of electrodes, thereby enhancing volumetric and areal energy densities while improving mechanical durability and fatigue resistance. Microstructural engineering, including multilayer helical winding and staggered alignment, can further extend ion transport

pathways and enlarge the electrochemically active surface area. Moreover, device design should ensure compatibility with textile manufacturing, wearable adaptability, and modular integration to enable scalable and reliable implementation in practical applications.

(2)Optimization of Electrode Materials and Electrolytes: The specific surface area, porosity, and zinc-storage capability of electrode materials are key factors governing the performance of fiber-based batteries. Nanostructuring, porosity engineering, and surface functionalization can create abundant active sites and accelerate electron/ion transport. Compositing with conductive carbon frameworks further improves electrochemical kinetics and structural stability. For electrolytes, highly conductive gel or solid-state systems enhance environmental adaptability and operational safety, while functional additives suppress dendrite growth and stabilize interfacial reactions. The integration of self-regulating electrolytes, bifunctional additives, and multiscale pore matching can further promote efficient electrode–electrolyte coupling. Systematic optimization of these parameters enables prolonged cycling stability and reliable performance under low temperature, high humidity, and dynamic mechanical conditions.

(3)Surface Coating and Doping Technologies: Constructing continuous conductive coatings such as carbon nanotubes, graphene, or conductive polymers enhances electron transport, lowers interfacial impedance, and promotes uniform Zn^{2+} deposition to suppress dendrite formation. Heteroatom doping with elements like Ni, Co, or Mn further tailors the crystal structure, adjusts electronic states, and improves ion diffusion kinetics and electrochemical stability. Introducing defect structures increases active sites, thereby boosting capacity and rate capability. Building on these strategies, integrating in situ regulation with multiscale interface engineering can yield electrodes with self-adaptive deposition behavior, enabling high power output and extended cycling life in fiber-based batteries.

(4)Innovation in Encapsulation Strategies: Encapsulation is vital for maintaining the flexibility, stability, and safety of fiber-based batteries. Multilayer or hierarchical designs enable functional partitioning, with the inner layer ensuring electrochemical stability and the outer layer providing mechanical protection and environmental isolation. Incorporating nanocoatings, hydrophobic layers, or self-healing polymers enhances durability and reliability under dynamic mechanical stress. Effective thermal management is also critical: thermally conductive layers or phase-change materials can regulate local temperature and mitigate performance degradation under extreme conditions. Integrating microstructured encapsulation with adaptive protection strategies establishes strong synergy between encapsulation and device architecture, ensuring reliable operation in wearable and outdoor applications.

(5)Enhancement of Environmental Adaptability: The stability of FFZIBs under extreme humidity and temperature remains a key challenge for practical applications. Corrosion-resistant metal oxides, hydrophobic carbon materials, and antifreeze or interference-tolerant electrolytes can maintain electrochemical performance and mechanical flexibility. Interface engineering using interfacial stabilizers or buffer layers strengthens electrode–electrolyte adhesion and mitigates performance degradation. Systematic optimization through multiphysical environmental simulations encompassing humidity, temperature, and mechanical stress can further refine materials, interfaces, and device structures. Looking forward, the development of environment-adaptive electrodes and electrolytes offers great potential for intelligent and stable operation of fiber-based batteries under complex and variable conditions.

(6)System Integration and Application Expansion: Future FFZIBs are expected to evolve from single-function energy storage units toward multifunctional, intelligent textile platforms. Incorporating self-healing or stimuli-responsive materials, such as electrochromic, thermoresponsive, or humidity-sensitive components, can impart damage-repair and environmental-sensing capabilities. Integration with sensors, light-emitting elements, or self-powered modules enables synergistic coupling of energy storage, information acquisition, and functional output. System-level design should consider flexible encapsulation, reliable electrical interconnection, and modular configurations to ensure performance and durability. The adoption of dynamic functional partitioning,

intelligent interconnectivity, and wearable health-monitoring functionalities will facilitate the development of high-performance, intelligent, and sustainable fiber-based electronic systems.

References

[1] P. Kulkarni, H. Kumar Beere, M. Jalalah, M. Alsaiari, R. Geetha Balakrishna, F. A. Harraz, D. Ghosh, Journal of Electroanalytical Chemistry 2022, 924, 116851.

[2] L. Liu, Y. Liu, J. Min, Q. Ding, Y. Fan, J. Yu, W. Jiang, Composites Communications 2024, 48, 101935.

[3] T. He, Q. Su, Z. Yildiz, K. Cai, Y. Wang, Electrochimica Acta 2016, 222, 1120-1127.

[4] S. Yang, S. Zhao, S. Chen, Chem Sci 2023, 14, 13346-13366.

[5] P. Bai, W. Tian, Z. Wang, G. Ling, J. Ren, R.-P. Ren, Y. Lv, Journal of Materials Science 2024, 59, 2437-2448.

[6] M. M. Ismail, Z.-Y. Hong, M. Arivanandhan, T. C.-K. Yang, G.-T. Pan, C.-M. Huang, Energies 2021, 14.

[7] Z. Guo, Y. Li, Z. Lu, Y. Chao, W. Liu, Journal of Materials Science 2022, 57, 3613-3628.

[8] W. Zhang, Z. Cao, Y. Li, R. Li, Y. Zheng, P. Su, X. Guo, Nanoscale 2024, 16, 9516-9524.

[9] M. Yang, G. Tao, M. Zhu, C. Hou, Advanced Fiber Materials 2025, 7, 351-353.

[10] T. Qin, H. Yang, Q. Li, X. Yu, H. Li, Industrial Chemistry & Materials 2024, 2, 191-225.

[11] K. Zhang, J. Z. Y. Wang, Journal of Electroanalytical Chemistry 2024, 953.

[12] L. Yang, Y. Zhao, Y. Dong, J. Yang, S. Wang, C. Wang, J. Bai, F. Xue, P. K. Chu, C. Chu, Surface and Coatings Technology 2025, 503.

[13] K. Wang, J. Wang, P. Chen, M. Qin, C. Yang, W. Zhang, Z. Zhang, Y. Zhen, F. Fu, B. Xu, Small 2023, 19, 2300585.

[14] P. Chen, W. Zhou, Z. Xiao, S. Li, Z. Wang, Y. Wang, S. Xie, Nano Energy 2020, 74, 104905.

[15] Y. Sun, J. Natsuki, S. Xu, P. Sun, W. Zhou, B. Li, W. Nie, T. Natsuki, Materials Letters 2024, 371, 136866.

[16] H. Zhang, T. Xiong, T. Zhou, X. Zhang, Y. Wang, X. Zhou, L. Wei, ACS Appl Mater Interfaces 2022, 14, 41045-41052.

[17] J. Xu, Z. Zhu, L. Hu, J. Wang, J. Liu, K. Yan, K. Zhu, Advanced Functional Materials 2025.

[18] J. Guo, B. He, W. Gong, S. Xu, P. Xue, C. Li, Y. Sun, C. Wang, L. Wei, Q. Zhang, Q. Li, Adv Mater 2024, 36, e2303906.

[19] X. Cheng, H. Gao, X. Tian, D. Wu, P. Lv, S. S. Yoon, J. Yang, Q. Wei, Nano Energy 2024, 125.

[20] N. Subjalearndee, N. He, H. Cheng, P. Tesatchabut, P. Eiamlamai, P. Limthongkul, V. Intasanta, W. Gao, X. Zhang, Advanced Fiber Materials 2022, 4, 457-474.

[21] Z. Xia, S. Li, G. Wu, Y. Shao, D. Yang, J. Luo, Z. Jiao, J. Sun, Y. Shao, Adv Mater 2022, 34, e2203905.

[22] C. Li, W. Wang, Y. Tang, W. Zhuang, J. Zhang, D. Zhang, X. Qian, G. Hong, J. Du, Y. Yao, J Colloid Interface Sci 2025, 677, 551-559.

[23] D. D. Khumujam, T. Kshetri, T. I. Singh, S. B. Singh, N. H. Kim, J. H. Lee, Chemical Engineering Journal 2024, 486.

[24] J. Pi, Y. Zhong, J. Zeng, H. Xu, P. Liao, G. Li, Y. Liao, Y. Qing, Y. Wu, Electrochimica Acta 2025, 527.

[25] J. Xu, N. Han, S. Chen, Y. Zhang, Y. Jing, Z. Chen, S. Wang, R. Chen, P. Bing, Z. Li, Journal of Energy Storage 2025, 120.

[26] J. Wu, J. Zhou, J. Guo, Y. Meng, Y. Xie, Y. Ling, B. Zheng, Z. Wang, Q. Zhang, Carbon 2024, 223.

[27] B. Ding, J. Tang, Z. Wang, Z. Liu, H. Xia, S. Wang, C. Li, Y. Zhang, H. Jia, X. Zheng, Colloids and Surfaces A: Physicochemical and Engineering Aspects 2025, 711.

[28] K. Wang, ACS Omega 2020, 5, 10225-10227.

[29] Q. Jian, J. Sun, H. Li, Z. Guo, T. Zhao, International Journal of Heat and Mass Transfer 2024, 223, 125252.

[30] Z. Shen, L. Luo, C. Li, J. Pu, J. Xie, L. Wang, Z. Huai, Z. Dai, Y. Yao, G. Hong, Advanced Energy Materials 2021, 11.

[31] Q. Guan, Y. Li, X. Bi, J. Yang, J. Zhou, X. Li, J. Cheng, Z. Wang, B. Wang, J. Lu, Advanced Energy Materials 2019, 9.

[32] S. Zhai, N. Wang, X. Tan, K. Jiang, Z. Quan, Y. Li, Z. Li, Advanced Functional Materials 2021, 31.

[33] F. Liu, S. Xu, W. Gong, K. Zhao, Z. Wang, J. Luo, C. Li, Y. Sun, P. Xue, C. Wang, L. Wei, Q. Li, Q. Zhang, ACS Nano 2023, 17, 18494-18506.

[34] Y. Shao, Z. Xia, L. Xu, X. Zhang, D. Yang, Z. Yang, J. Luo, G. Xiao, Y. Yang, Y. Su, G. Lu, J. Sun, T. Cheng, Y. Shao, Adv Mater 2024, 36, e2407143.

[35] T. Chen, Y. Wang, Y. Yang, F. Huang, M. Zhu, B. T. W. Ang, J. M. Xue, Advanced Functional Materials 2021, 31.

[36] T. Li, Q. Xu, M. Waqar, H. Yang, W. Gong, J. Yang, J. Zhong, Z. Liu, Energy Storage Materials 2023, 55, 64-72.

[37] J. Pu, Q. Cao, Y. Gao, Q. Wang, Z. Geng, L. Cao, F. Bu, N. Yang, C. Guan, Adv Mater 2024, 36, e2305812.

[38] Z. Wang, D. Zhou, Z. Zhou, W. Gong, S. Zhao, Y. Ling, F. Liu, J. Guo, K. Zhao, J. Wu, P. Xue, C. Li, Y. Sun, J. Luo, Z. Wang, J. Xu, L. Wei, Q. Zhang, Advanced Functional Materials 2024, 34.

[39] M. Lin, R. Qi, W. Zhang, Z. Ren, J. Si, Q. Lei, Y. Sun, H. Li, J. He, Q. Zhang, J. Zeng, W. Wen, Y. Gao, X. Li, D. Zhu, Advanced Energy Materials 2024, 14.

[40] Z. Cong, W. Guo, P. Zhang, W. Sha, Z. Guo, C. Chang, F. Xu, X. Gang, W. Hu, X. Pu, ACS Applied Materials & Interfaces 2021, 13, 17608-17617.

[41] L. Sha, B.-B. Sui, P.-F. Wang, Z. Gong, Y.-H. Zhang, Y.-H. Wu, L.-N. Zhao, J.-J. Tang, F.-N. Shi, Chemical Engineering Journal 2024, 481.

[42] S.-J. Guo, M.-Y. Yan, D.-M. Xu, P. He, K.-J. Yan, J.-X. Zhu, Y.-K. Yu, Z.-Y. Peng, Y.-Z. Luo, F.-F. Cao, Energy & Environmental Science 2025, 18, 418-429.

[43] H. Tian, M. Yao, Y. Guo, Z. Wang, D. Xu, W. Pan, Q. Zhang, Advanced Energy Materials 2024, 15.

[44] X. Wang, P. Lei, C. Zheng, Z. Wang, B. Wang, X. Cui, J. Cheng, Advanced Functional Materials 2025.

[45] S. Xu, P. Shen, Z. Shen, R. Chen, D. Zhang, Z. Zhao, Y. Zhang, D. Li, Y. Xiong, X. Wang, Y. Hu, J. Zhao, Chemical Engineering Journal 2025, 504.

[46] K. Zhu, J. Luo, D. Zhang, N. Wang, S. Pan, S. Zhou, Z. Zhang, G. Guo, P. Yang, Y. Fan, S. Hou, Z. Shao, S. Liu, L. Lin, P. Xue, G. Hong, Y. Yang, Y. Yao, Adv Mater 2024, 36, e2311082.

[47] C. Li, W. Wang, J. Luo, W. Zhuang, J. Zhou, S. Liu, L. Lin, W. Gong, G. Hong, Z. Shao, J. Du, Q. Zhang, Y. Yao, Adv Mater 2024, 36, e2313772.

[48] G.-Y. Wang, G.-X. Li, Y.-D. Tang, Z. Zhao, W. Yu, C.-Z. Meng, S.-J. Guo, The Journal of Physical Chemistry Letters 2023, 14, 3512-3520.

[49] J. Liu, N. Nie, J. Wang, M. Hu, J. Zhang, M. Li, Y. Huang, Materials Today Energy 2020, 16.

[50] G. Shim, M. X. Tran, G. Liu, D. Byun, J. K. Lee, Energy Storage Materials 2021, 35, 739-749.

[51] H. Yu, G. Liu, M. Wang, R. Ren, G. Shim, J. Y. Kim, M. X. Tran, D. Byun, J. K. Lee, ACS Applied Materials & Interfaces 2020, 12, 5820-5830.